


Protection of the Vascular System by Polyethylene Glycol Reduces Secondary Injury Following Spinal Cord Injury in Rats

Jinseung Lee^{1,2,3} · Suk-Chan Hahm⁴ · Heayeon Yoo^{1,2} · Young Wook Yoon⁵ · Junesun Kim^{1,2,3,6} 

Received: 4 November 2022 / Revised: 11 May 2023 / Accepted: 21 June 2023 / Published online: 12 September 2023
© Korean Tissue Engineering and Regenerative Medicine Society 2023

Abstract

BACKGROUND: Polyethylene glycol (PEG) is a hydrophilic polymer, which has been known to have a neuroprotective effect by sealing the ruptured cell membrane, but PEG effects on the vascular systems and its underlying mechanisms remain unclear. Here, we showed the neuroprotective effect of PEG by preventing damage to the vascular system.

METHODS: A spinal contusion was made at the T11 segment in male Sprague–Dawley rats. PEG was injected into the subdural space immediately after SCI. Vascular permeability was assessed for 24 h after SCI using intraperitoneally injected Evans blue dye. Junctional complexes were stained with CD31 and ZO-1. Infarct size was analyzed using triphenyltetrazolium chloride, and blood vessels were counted in the epicenter. Behavioral tests for motor and sensory function were performed for 6 weeks. And then the tissue-sparing area was assessed.

RESULTS: Immediately applied PEG significantly reduced the vascular permeability at 6, 12, and 24 h after SCI when it compared to saline, and infarct size was also reduced at 0, 6, and 24 h after SCI. In addition, a great number of blood vessels were observed in PEG group at 6 and 24 h after SCI compared to those of the saline group. The PEG group also showed a significant improvement in motor function. And tissue-sparing areas in the PEG were greater than those of the saline group.

CONCLUSION: The present results provide preclinical evidence for the neuroprotective effects of PEG as a promising therapeutic agent for reducing secondary injury following SCI through vascular protection.

Keywords Polyethylene glycol · Spinal cord injury · Vascular system

✉ Junesun Kim
junokim@korea.ac.kr

¹ Rehabilitation Science Program, Department of Health Science, Graduate School, Korea University, Seoul 02841, Korea

² Transdisciplinary Major in Learning Health Systems, Department of Healthcare Sciences, Graduate School, Korea University, Seoul 02841, Korea

³ Department of Physical Therapy, Undergraduate School, Korea University College of Health Science, Anam-dong, Sungbuk-gu, Seoul 02841, Korea

⁴ Graduate School of Integrative Medicine, CHA University, Seongnam 13488, Korea

⁵ Department of Physiology, Korea University College of Medicine, Seoul 02841, Korea

⁶ Department of Health and Environmental Science, Undergraduate School, Korea University College of Health Science, Seoul 02841, Korea

1 Introduction

Spinal cord injury (SCI) is an incurable disease with biphasic pathological processes; namely, primary injury caused by direct insult to the spinal cord and secondary injury due to a degenerative neural response after injury [1–3]. The initiation of secondary injury results from primary trauma; its progression is affected by microenvironmental changes related to ischemia, inflammation, and immune response [4, 5]. Among these, the dysfunction of the vascular system contributes to secondary injury initiation and progression [6–8].

The vascular mechanisms in traumatic SCI include disruption of the blood-spinal cord barrier (BSCB), which functions equally to the blood–brain barrier and provides a controlled extracellular environment. The function of the BSCB in controlling vascular permeability is based on a complex of endothelial cells (ECs), pericytes, astrocytes, and other accessory structures, such as the basement membrane, that play regulatory and protective roles in spinal tissues [9]. Breakdown of the BSCB increases hemorrhage, including the indiscriminate leakage of toxic factors such as blood cells, calcium ions, excitatory factors, free radicals, and inflammatory mediators [10–16]. These leakages contribute to secondary injury, including the self-degeneration of neurons and glial cells [17, 18]. Given the implications of BSCB dysfunction in secondary injury, it is important to control permeability after SCI.

Polyethylene glycol (PEG) is a hydrophilic polymer with biocompatibility and fusogenic properties that may have neuroprotective effects [19, 20]; however, the underlying mechanisms of these effects are unclear. One possible mechanism is the membrane-sealing effect of PEG. PEG can anatomically repair crushed nerve membranes and reverse membrane permeability while preserving membrane integrity in the spinal cord [21–23]. This sealing effect is related not only to the prevention or repair of damaged spinal tissues but also to the recovery of neurological function. Borgens and Shi [24] demonstrated immediate axonal repair and functional recovery with the application of PEG after a clipping injury based on observations of the cutaneous trunci muscle reflex and somatosensory-evoked potential. Baptiste et al. [25] reported the systemic application of PEG preserved membrane integrity to reduce secondary injury and improve neurological function. However, the therapeutic effect of PEG on vascular protection to reduce secondary damage following SCI has not been studied. We hypothesized that the vascular sealing effects of PEG would reduce secondary damage following SCI.

Thus, in the present study, we investigated the effects of PEG on secondary injury following SCI-induced vascular

damage by examining vascular permeability, infarct size, blood vessel number, motor-sensory functions, and tissue-sparing at the lesion site following the immediate application of PEG after SCI in rats.

2 Materials and methods

2.1 Animals and ethics

All procedures were approved by the Korea University Institutional Animal Care and Use Committee (KUIACUC-2019–0016). Adult male Sprague–Dawley rats (8-week-old; 200–220 g; $n = 81$; Orient Bio Inc., Seoul, Korea) were used in this study. In this study, male rats were used to avoid cyclic hormonal changes in female rats. The animals were kept under a 12 h/12 h light–dark cycle (08:00–20:00) with free access to water and food.

2.2 Experimental design

We investigated the changes in the vascular system during the acute phase after SCI in rats and the neuroprotective effects of PEG for 6 weeks after contusive SCI (Fig. 1). First, the rats were randomly divided into two groups: 1) SCI rats receiving saline (saline group, $n = 33$) and 2) SCI rats receiving PEG (experimental group, $n = 33$). Each group was randomly divided into five groups to investigate the time-dependent changes in BSCB function (0, 3, 6, 12, and 24 h after SCI) and three groups to confirm the infarct size after SCI (0, 6, and 24 h after SCI) (Fig. 1A). To calculate the percentage of infarct size spinal tissues of naïve rats were used ($n = 3$). For the analysis of junctional complexes of the vascular system and blood vessels, we used the spinal tissues of rats to confirm EBD signals. Second, behavioral assessments were performed for 6 weeks in the saline ($n = 6$) and PEG ($n = 6$) groups (Fig. 1B). Behavioral assessments were conducted before and after the SCI (before and after PEG or saline injection).

2.3 Surgical procedures and postoperative care

Contusive SCI was performed at the T11 spinal segment using a New York University impactor (New York University, New York, USA) [26]. A laminectomy was performed only on T10 under deep anesthesia with isoflurane (3% isoflurane and 97% O₂). The spinal column was fixed by clamping the T9 and T11 spinous processes with tissue forceps. A rod (10 g in weight) was dropped directly onto the exposed spinal cord (targeting the T11 spinal segment) from a height of 12.5 mm. The muscles and skin were sutured, and the animals were allowed to recover from anesthesia. Their bladders were manually

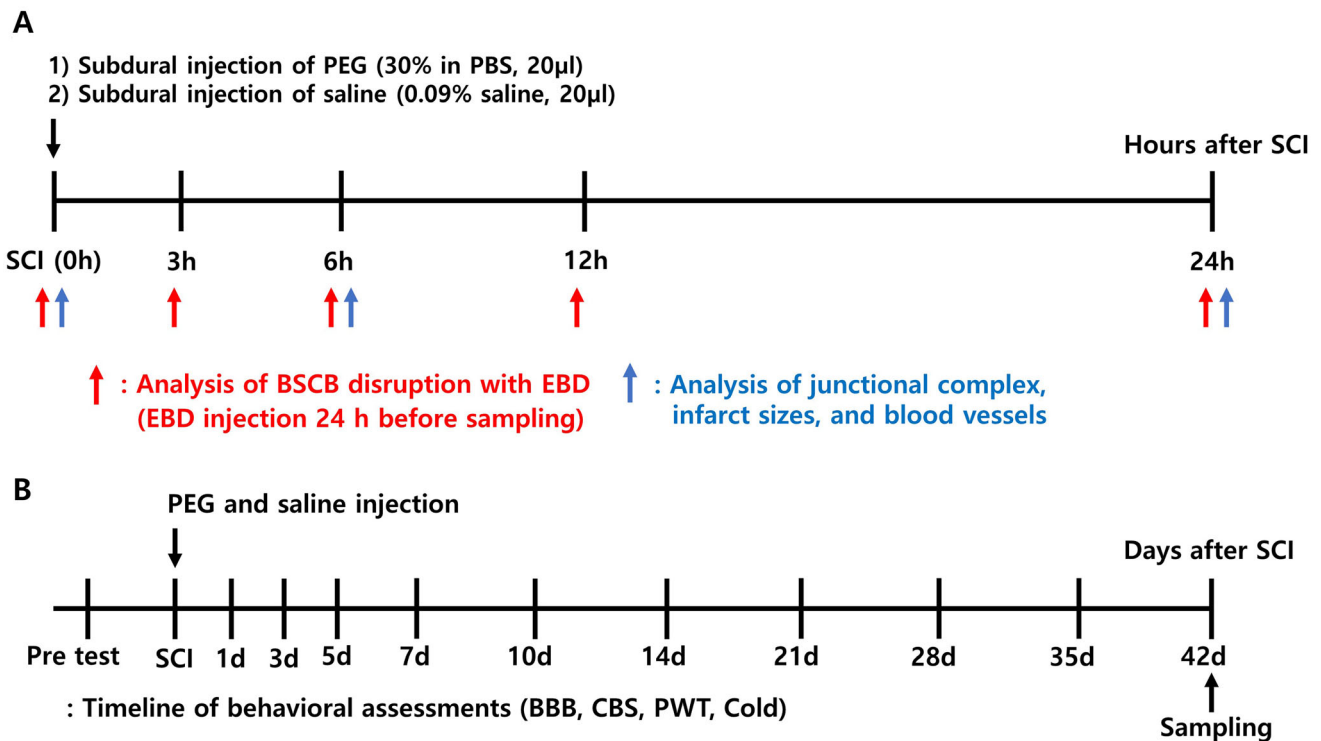


Fig. 1 Experiment timeline. Experimental design to assess the effects of PEG on secondary injury after SCI in rats. PEG or saline was injected into the dura mater in each group immediately after SCI. In experiment **A**, The red arrows show the timeline of the analyses of BSCB disruption. EBD was injected 24 h before sampling, contusive SCI was performed on the spinal cord, and samples were extracted at 0 h, 3 h, 6 h, 12 h, and 24 h after SCI ($n = 3$ at each time point). The blue arrows show the timeline of the analyses of the junctional

complex, infarct sizes ($n = 6$ at each time point), and blood vessels in the spinal cord ($n = 3$ at each time point). In experiment **B**, the motor-sensory function was quantified using the BBB, CBS, PWT, and cold tests before and after injury and assessed for 42 days after SCI ($n = 6$ in each group). PEG, polyethylene glycol; SCI, spinal cord injury; EBD, Evans blue dye; BBB, Bresnahan locomotor rating scale; CBS, modified combined behavioral score; PWT, paw withdrawal threshold; Cold, cold test

expressed twice daily until spontaneous urination was achieved. Unasyn (ampicillin/sulbactam, 100 mg/kg; Pfizer, Seoul, Korea) was injected intraperitoneally twice daily to prevent urinary tract infection.

2.4 Administration of PEG

To determine the neuroprotective effect of PEG on the vascular system following contusive SCI, 30% PEG in phosphate-buffered saline (PBS) (MW 600, 20 μ L, Sigma-Aldrich, St Louis, MO) was injected under the dura mater of the epicenter (T11) immediately after SCI in the PEG group, while saline (0.9% in PBS, 20 μ L) was injected in the saline group. Low molecular weight PEG was selected for its biocompatibility and property of negligible immune response in spinal cord [27]. PEG was administered under the dura mater using a 50 μ L Hamilton syringe without further disruption of the dura mater and bleeding during the injection. PEG was delivered slowly to avoid volume damage at the injury site.

2.5 Analysis of alterations in BSCB function

To examine the effects of PEG application on the degree of destruction of the BSCB after SCI, we performed quantitative and morphological evaluations of vascular permeability using Evans blue dye (EBD), which has low permeability to the extracellular matrix (ECM) in the normal state [28]. EBD (1% in PBS, 1 ml/100 g, Sigma-Aldrich) solution was administered intraperitoneally (IP) 24 h before tissue sampling. For extraction, the rats were perfused with 0.9% saline 4% paraformaldehyde (pH 7.4) under deep anesthesia with sodium pentobarbital (50 mg/kg, IP). Spinal segments (T10–T12) were extracted following the time courses (0, 3, 6, 12, and 24 h after SCI) for each group. After extraction, spinal tissues were post-fixed with 4% paraformaldehyde at 4 $^{\circ}$ C overnight and dehydrated with 30% sucrose. Then tissues were embedded into the optimal cutting temperature (OCT) compound and frozen. Spinal tissues were sectioned longitudinally for analyzing the area of EBD extravasation. Because EBD is fluorescently expressed, EBD extravasation was examined

with its expression using a Leica DM 2500 (Leica Microsystems GmbH, Wetzlar, Germany) and a Leica Camera DFC 450C (Leica Microsystems GmbH) for image capture. To investigate the total tendency of BSCB destruction around the epicenter, EBD extravasation in three segments of spinal tissues containing the epicenter in the middle was analyzed. For the analysis, we measured the area near the corticospinal tract (CST) where the dorsal horn began to appear and calculated the area where EBD was fluorescently expressed with NIH Image software (National Institutes of Health, Bethesda, MD, USA). The distance of EBD extravasation was also analyzed from the rostral-most point to the caudal-most point with NIH Image software. For the analysis of the area and distance of EBD extravasation, five samples were analyzed in each rat.

2.6 Analysis of junctional complexes

For changes in vascular structures, junctional complexes were investigated around the epicenter. CD31 and ZO-1 were used to stain blood vessels and junctional proteins [29, 30]. Sectioned tissues at 0, 6, and 24 h after SCI were used for immunohistochemical staining. The sections were washed with PBS to remove the OCT compound, permeabilized with 0.5% Triton X-100 for 15 min at room temperature, and blocked with avidin and biotin (Vector Laboratories, Burlingame, CA, USA). The sectioned tissues were incubated with the following primary antibodies overnight at 4 °C: rabbit anti-CD31 (1:2000, Abcam, Cambridge, UK) and mouse anti-ZO-1 (1:1000, Invitrogen Life Technologies, Carlsbad, CA, USA). Tissues were then incubated with secondary antibodies for 1 h at room temperature: biotinylated goat anti-rabbit immunoglobulin G (IgG, 1:1000, Vector Laboratories) and biotinylated goat anti-mouse IgG (1:1000, Vector Laboratories), followed by Alexa Fluor 405 (1:1000, Jackson ImmunoResearch, West Grove, PA, USA) and Alexa Fluor 488 (1:1000, Invitrogen Life Technologies) 1 h at room temperature. The images of CD31 and ZO-1 were merged with EBD signals. The areas of CD31 and ZO-1 were the edges of the epicenter of the white matter.

2.7 Alteration of infarct size in spinal tissues

The infarct size was calculated by triphenyl tetrazolium chloride (TTC; Sigma-Aldrich) staining. The spinal tissues (T10–T12) were extracted at 0, 6, and 24 h after SCI. The process of extraction was mentioned above. The extracted spinal tissues were semi-frozen before slicing into 2.0-mm transverse sections. Three segments were analyzed (rostral, epicenter, and caudal). The sections were incubated in 2% TTC in PBS for 30 min at 37 °C, then transferred to 4% paraformaldehyde for fixation. Because TTC stains

dehydrogenases in the mitochondria, stained areas exist mainly in the gray matter of the spinal cord. Therefore, we defined the non-stained tissue of gray matter as the infarction area. Additionally, dark and rough surfaces of the gray matter were also defined as the infarction area owing to cavitation caused by cell death. The infarct sizes were measured using NIH Image. The averages of the three segments were calculated and shown as the percentages of the stained areas of the injured rat in the spinal tissue of naïve rats.

2.8 Blood vessel morphometry and image analysis

To analyze blood vessel destruction, we used the same samples which were used for the analysis of EBD extravasation. Based on EBD extravasation after SCI, tissues at 0, 6, and 24 h after SCI, when a dramatic change in BSCB function occurred, were analyzed. The blood vessels were stained with laminin (Sigma-Aldrich), which is commonly used to analyze blood vessels in the central nervous system [31]. The sections were washed with PBS to remove the OCT compound, blocked with 10% normal goat serum (NGS) for 1 h at room temperature, and incubated in primary antibody: rabbit anti-laminin (1:2000). After washing, the tissue sections were incubated with a secondary antibody (biotinylated goat anti-rabbit immunoglobulin G [IgG], 1:1000 Vector Laboratories) for 1 h. The tissues were then incubated with ABC agent (Vector Laboratories) and DAB peroxidase substrate kit (Vector Laboratories) and dehydrated with alcohol dipped in xylene. For analysis, two experimenters blinded to the treatment groups manually counted the blood vessels at the lesion sites. To discriminate stained blood vessels from cell basal lamina or background [31], only tubular and ring-like structures were analyzed manually by creating a skeletal line with a basic sketch program. After sketching, the images were converted to 8-bit black-and-white images to easily capture skeletal lines and count blood vessels.

2.9 Behavioral assessments

2.9.1 Motor function

Motor recovery of the animals after SCI was evaluated before and at 1, 3, 5, 7, 10, 14, 21, 28, 35, and 42 d after SCI. The Basso, Beattie, and Bresnahan locomotor rating scale (BBB) [32] and modified combined behavioral score (CBS) [33] were used to assess hindlimb motor function. The BBB is a 21-point open-field locomotion test commonly used to confirm locomotor functions in rats. In the CBS, there are one test for recovery of gross motor function and four tests for recovery of reflexes (spreading to toes elicited by being lifted, returning to an upright position

in response to being rolled over on the back, withdrawing the hindlimb by flexion in response to being manually extended, and placing the hind foot upon a table in response to the tactile stimulus on the dorsal surface of the hind paw).

2.9.2 Mechanical sensitivity

Mechanical sensitivity was assessed by paw withdrawal threshold (PWT) with a series of eight different von Frey filaments with logarithmically increasing stiffness (0.41–15.10 g) (Stoelting, Wood Dale, IL, USA using the up and down method [34] beginning with the 2.0 g (4.31 mN) filament in the middle of the series. A brisk paw withdrawal response accompanied by a complex supraspinal behavior, such as attention, licking, vocalization, and postural change, was regarded as a positive response.

2.9.3 Cold test

To evaluate the change in sensitivity to cold stimulation, the frequency of brisk paw withdrawal response to the application of 100% acetone to the plantar surfaces of both hind paws was measured. The test procedures have been described previously [35]. Briefly, acetone was applied five times at 5-min intervals to each paw. The frequency of paw withdrawal was expressed as a percentage: # of paw withdrawal responses/total # of trials \times 100.

2.10 Morphometric assessment of tissue-sparing

To examine the difference in tissue-sparing of spinal cord after PEG or saline application, spinal segments (T10–T12) were extracted, post-fixed overnight with 4% paraformaldehyde, and transferred to 30% sucrose for cryoprotection. The tissues were then embedded in OCT compound for cryosection, longitudinally sectioned (12 μ m) on a cryostat microtome, and serially attached to the slides for analysis. The sectioned tissues were stained with 0.1% Luxol Fast Blue (LFB, ACROS Organics, Maybridge, Fisher Chemical) for myelin sheath staining and 0.1% cresyl violet (Sigma-Aldrich) for Nissl staining. Five samples in each rat were analyzed with NIH image software.

2.11 Statistical analysis

Statistical analyses were performed using the software IBM SPSS Statistics for Windows, version 26.0 (IBM Corp., Armonk, NY, USA). The values are shown as means \pm standard error of the mean (SEM). For the statistical analysis of the behavioral assessments including BBB, CBS, PWT, and cold test results from animals with contusive SCI, data were calculated from the average of

each hind limb. The Mann–Whitney U test was performed to investigate the changes in EBD extravasation, infarct size, and the number of blood vessels in two groups. For behavioral differences, to compare the difference between two groups in the same time point, Mann–Whitney U was also used. The alpha level was set to 0.05.

3 Results

3.1 Protective effect of PEG on BSCB destruction following SCI

Immediately after SCI, EBD leakage in the spinal cord was started in the saline group. After then, EBD extravasation increased in the epicenter and was extended to the rostral and caudal segments depending on the time after SCI. EBD extravasation dramatically increased between 3 h after SCI and peaked at 24 h after SCI in the saline group. However, EBD extravasation in the PEG group was remarkably lower than that in the saline group for most of the time points (6 h: $p = 0.000007$; 12 h: $p = 0.000323$; 24 h: $p = 0.0000004$) (Fig. 2K).

To test the degree of BSCB breakdown, the distance of EBD extravasation from the rostral to the caudal segments (Fig. 2L) was analyzed. In the saline group, the leaked EBD rapidly spread to the rostral and caudal segments in the early phase; however, the PEG group showed a significantly decreased EBD extravasation from 3 to 6 h (3 h: $p = 0.056$; 6 h: $p = 0.001$) after SCI (Fig. 2L). The distance of EBD extravasation from the rostral to the caudal segments drastically increased 3 h after SCI in the saline group, however, but the PEG group showed a delayed increase in EBD extravasation at 12 h after SCI.

3.2 Alteration of junctional complexes after PEG application

The junctional complexes of the vascular structures were stained with CD31 and ZO-1, which did not differ immediately after SCI. At this time point, ZO-1 signals were rarely expressed, and CD31 signals around the epicenter were usually merged with EBD signals in both groups (Fig. 3A). After 6 h of SCI, the intensity of ZO-1 signals increased in the PEG group. The junctional complexes, which were the merged locations of CD31 and ZO-1, were found only in the PEG group. The distributions of junctional complexes were shown in Fig. 3D which was an image of 3 spinal segments 6 h after SCI in PEG group. In Fig. 3D, EBD signals in both groups were mainly fluorescently expressed at the epicenter, and CD31 and ZO-1 signals were not discriminated. CD31 and ZO-1 signals were mainly observed at the margin of the epicenter in both groups. In case of saline group, the analyzed

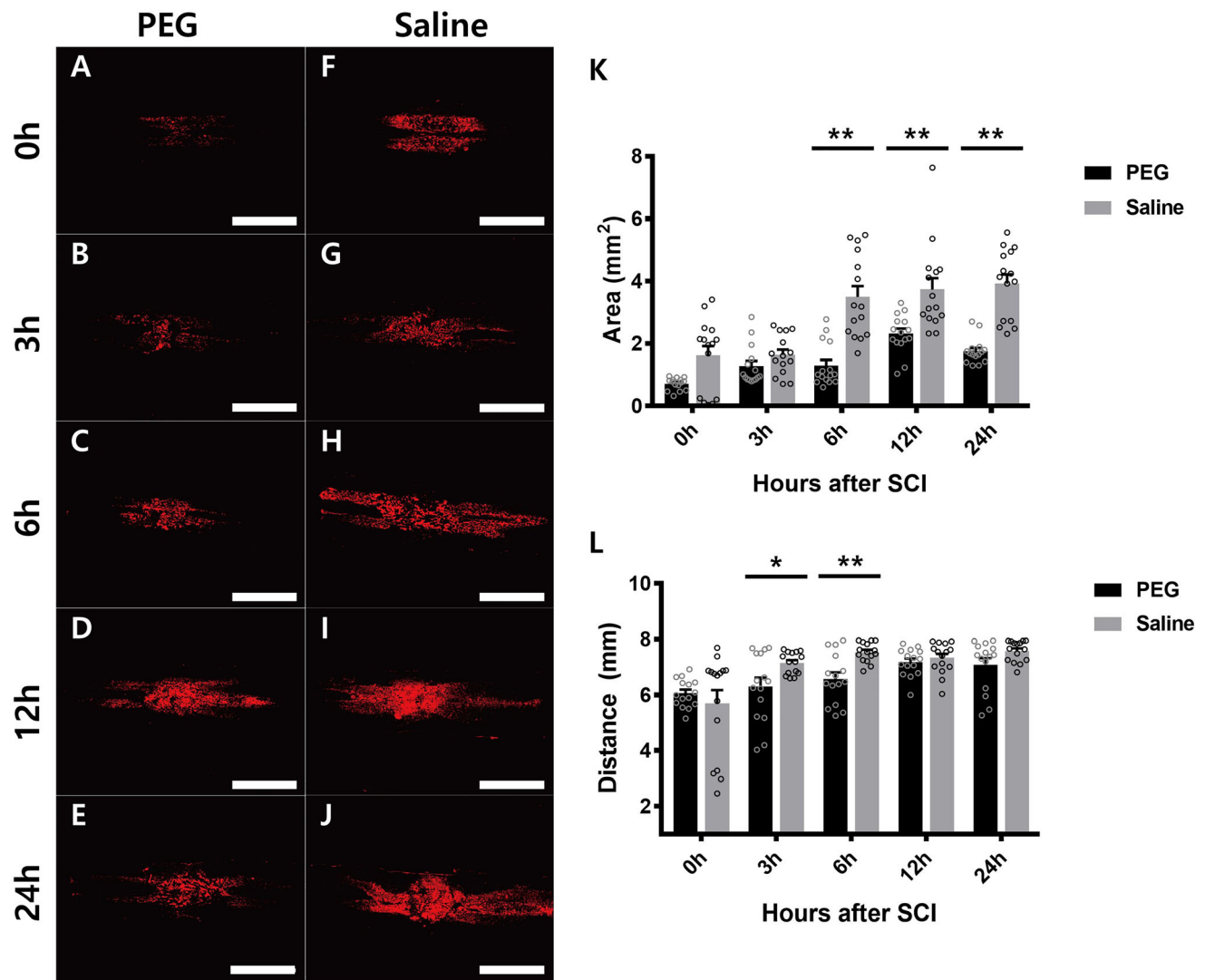


Fig. 2 Comparisons of EBD extravasation between the PEG and saline groups. **A–E** Changes in EBD extravasation following SCI in the PEG group (A: 0 h, B: 3 h, C: 6 h, D: 12 h, and E: 24 h after SCI). **F–J** Changes in EBD extravasation following SCI in the saline group (F: 0 h, G: 3 h, H: 6 h, I: 12 h, and J: 24 h after SCI). **K** Areas of EBD extravasation after SCI, showing that PEG injection significantly decreased EBD extravasation compared to saline

area was farther from epicenter compared to the PEG group because of the injured area. The stained junctional complexes were also observed in the PEG group 24 h after SCI (Fig. 3C). However, in the saline group, no spinal tissue showed a merged image of CD31 and ZO-1 6 h after SCI, and junctional complexes were found only 24 h after SCI (Fig. 3C).

3.3 Infarct size

The infarct size of the spinal segments was analyzed according to the time after SCI (Fig. 4C). In the epicenter tissues, the ischemic injury was observed in all tissues from 0 to 24 h after SCI. Depending on the time up to 24 h after

injection. **L** Distances of EBD extravasation. Asterisk (*) indicates values that differ significantly between the PEG and saline groups ($p < 0.05$) and Double-Asterisk (**) indicates values that differ significantly between the PEG and saline groups ($p < 0.01$). Scale bar: **A–J** 2 mm. EBD, Evans blue dye; PEG, polyethylene glycol; SCI, spinal cord injury

SCI, the infarction area extended to the rostral and caudal sites in both groups, and the surfaces of the spinal cord showed a rough appearance due to cavitation. The caudal segments were more affected by ischemic injury than rostral segments in the saline group (Fig. 4B). However, the PEG group showed a significantly reduced infarct size in the spinal tissues compared to the saline group (0 h: $p = 0.002$; 6 h: $p = 0.002$; 24 h: $p = 0.015$).

3.4 Effect of PEG on blood vessel destruction

To investigate blood vessel alteration, blood vessels were counted at the epicenter after SCI (Fig. 5). Immediately

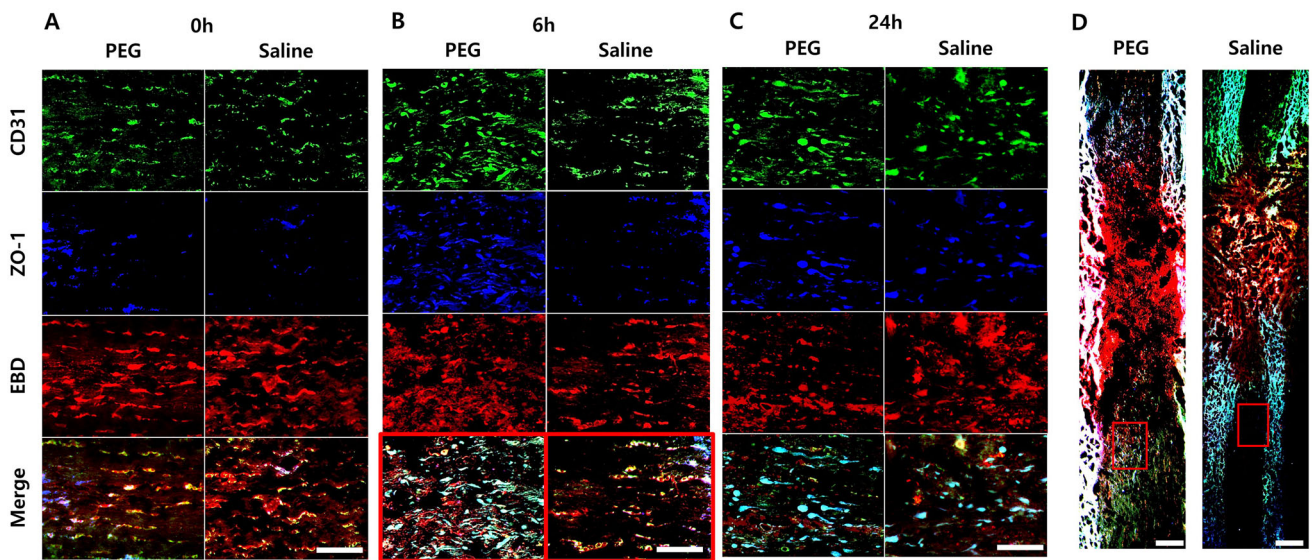


Fig. 3 The effect of PEG application on the structure of junctional complexes. **A–C** Stained tissues with CD31 and ZO-1 merged with EBD signals around the epicenter **A**: 0 h, **B**: 6 h, and **C**: 24 h in PEG and saline groups. The left side images in each **A**, **B**, and **C** show the stained tissues in the PEG group and the right shows the stained tissues in the saline group. **D** Longitudinal image of spinal cord

expressing EBD signals and stained with CD31 and ZO-1 6 h after SCI in the PEG and saline groups. The red box in **D** indicates the location of images in the 6 h after SCI in the PEG and saline groups. Scale bar: **A–C** 100 μ m, **D** PEG group: 100 μ m, saline group 200 μ m. EBD, Evans blue dye; PEG, polyethylene glycol; SCI, spinal cord injury

after SCI, there was no significant difference in the degree of blood vessel destruction between the PEG and saline groups (Fig. 5C). The blood vessels replacing the injured parenchyma were observed in the PEG group from 6 h after SCI. The numbers of blood vessels that newly replaced the lesion site were significantly higher at 6 h and 24 h after SCI (6 h: $p = 0.011$; 24 h: $p = 0.024$) in the PEG group (Fig. 5C), with a maximal gap between the two groups at 6 h after SCI. In the saline group, the blood vessels were also observed in the injured epicenter but was

delayed and showed a small increase in the number of new blood vessels.

3.5 Recovery of motor-sensory functions

To determine the effect of PEG on neurological function, we assessed motor and sensory function after SCI. The PEG group showed significant recovery in locomotor activity (BBB) during the experimental period compared to the saline group (3 d: $p = 0.041$; 5 d: $p = 0.015$; 7 d:

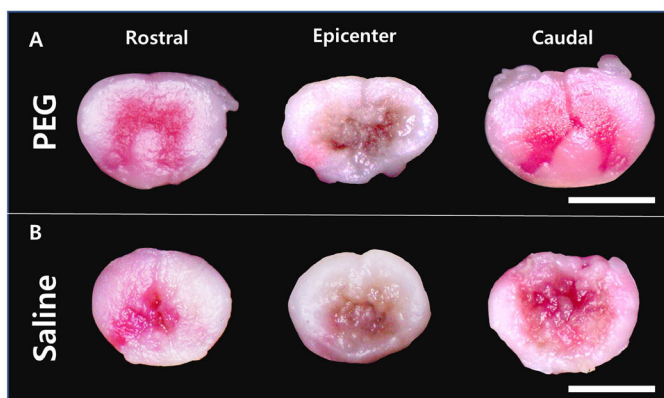
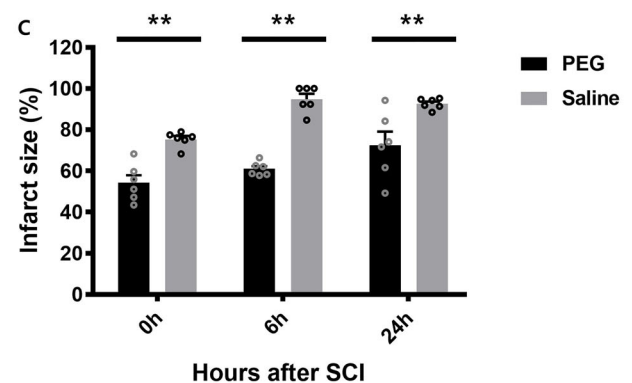


Fig. 4 Comparisons of infarct size in spinal tissues between the PEG and saline groups. TTC-stained spinal tissues, including the rostral, epicenter, and caudal segments in the PEG **A** and saline **B** groups 6 h after SCI, in which unstained areas indicate infarctions. The infarct sizes were measured as the percentage of the stained area in injured tissue to the area of the normal tissue. Each stained area was



calculated as the average of three spinal tissue segments. **C** Graph of infarct size 0 h, 6 h, and 24 h after SCI. Double-Asterisk (**) indicates values that differ significantly between the PEG and saline groups ($p < 0.01$). Scale bar: **A** and **B** 5 mm. TTC, triphenyl tetrazolium chloride; PEG, polyethylene glycol; SCI, spinal cord injury

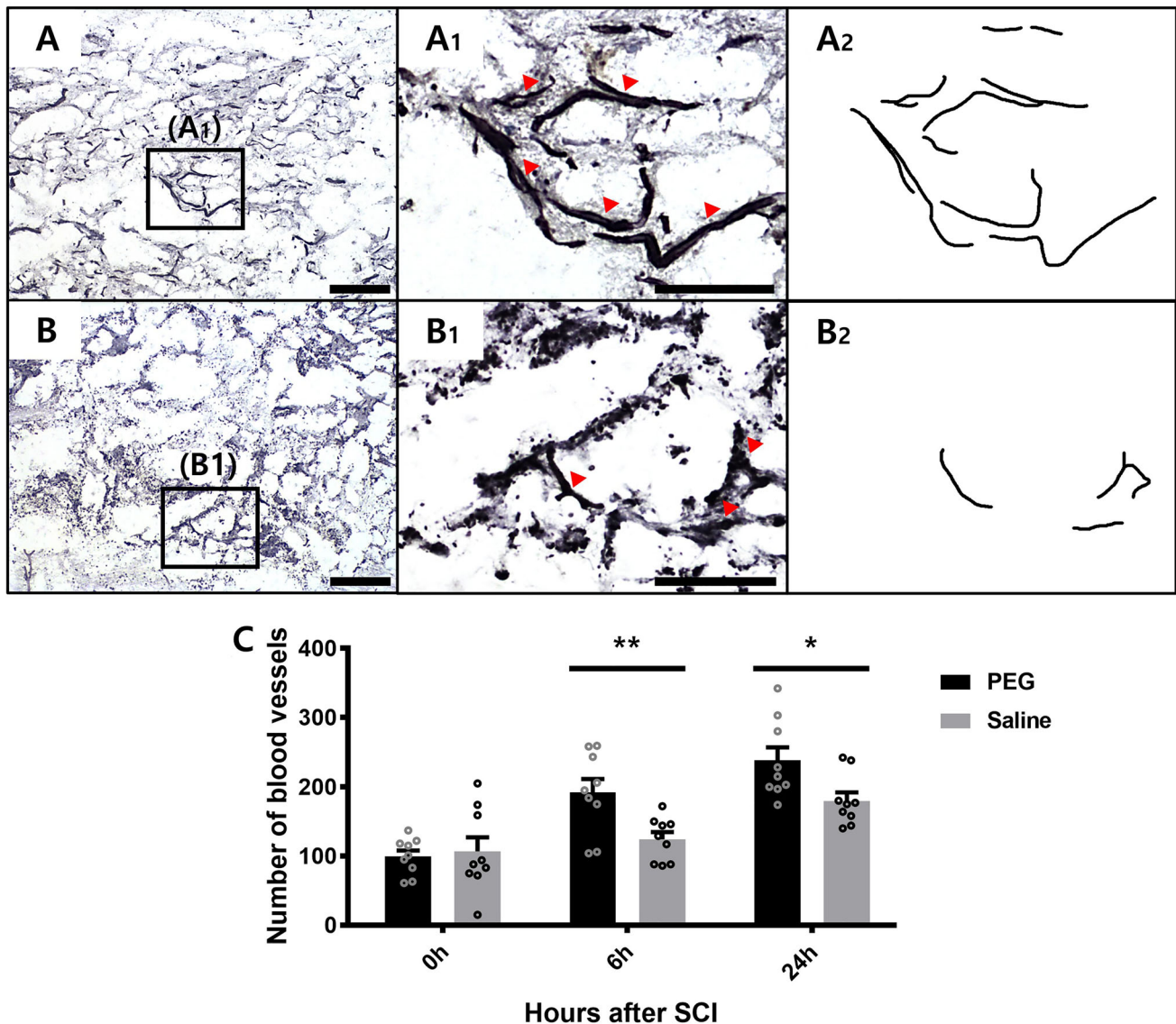


Fig. 5 Comparisons of blood vessels alterations at the lesion sites between the PEG and saline groups **A** and **B**. Blood vessels stained with laminin at lesion sites 6 h after SCI after PEG **A** and saline **B** injections. **A₁** and **B₁** Higher magnification of the boxes in **A** and **B** for indicating stained blood vessels. Red arrows in **A₁** and **B₁** indicate the stained blood vessels. **A₂** and **B₂** Skeletonized images of **A₁** and **B₁**. **C** Numbers of blood vessels stained with laminin at the

lesion sites based on the skeletonized images. Asterisk (*) indicates values that differ significantly between the PEG and saline groups ($p < 0.05$) and Double-Asterisk (**) indicates values that differ significantly between the PEG and saline groups ($p < 0.01$). Scale bar: **A** and **B** 200 μm , **A₁** and **B₁** 100 μm . PEG, polyethylene glycol; SCI, spinal cord injury

$p = 0.041$; 14 d: $p = 0.004$; 28 d: $p = 0.026$; 35 d: $p = 0.015$; 42 d: $p = 0.041$) (Fig. 6A). In particular, all rats in the PEG group could bear their body weight (BBB > 9), whereas some rats in the saline group could not bear their weight in the chronic phase after SCI. The earlier improvement of motor function in the PEG group was maintained for 6 weeks after SCI. The CBS score in the PEG group was lower than the saline group, suggesting that the degree of motor recovery in the PEG group was greater through the end of the experiment. However, there were

significant differences between the PEG and saline groups only at 1 and 3 days after SCI (1 d: $p = 0.015$; 3 d: $p = 0.004$) (Fig. 6B). In both groups, most rats spontaneously recovered the decreased reflexes except the reflex to the tactile stimulus on the dorsal surface of the hind paw accompanied with recovery of locomotor function following SCI.

In the sensory function, following SCI, rats did not respond to mechanical stimuli and PWT was maintained 15 g up to 3 days after injury. From 5 days after SCI, rats

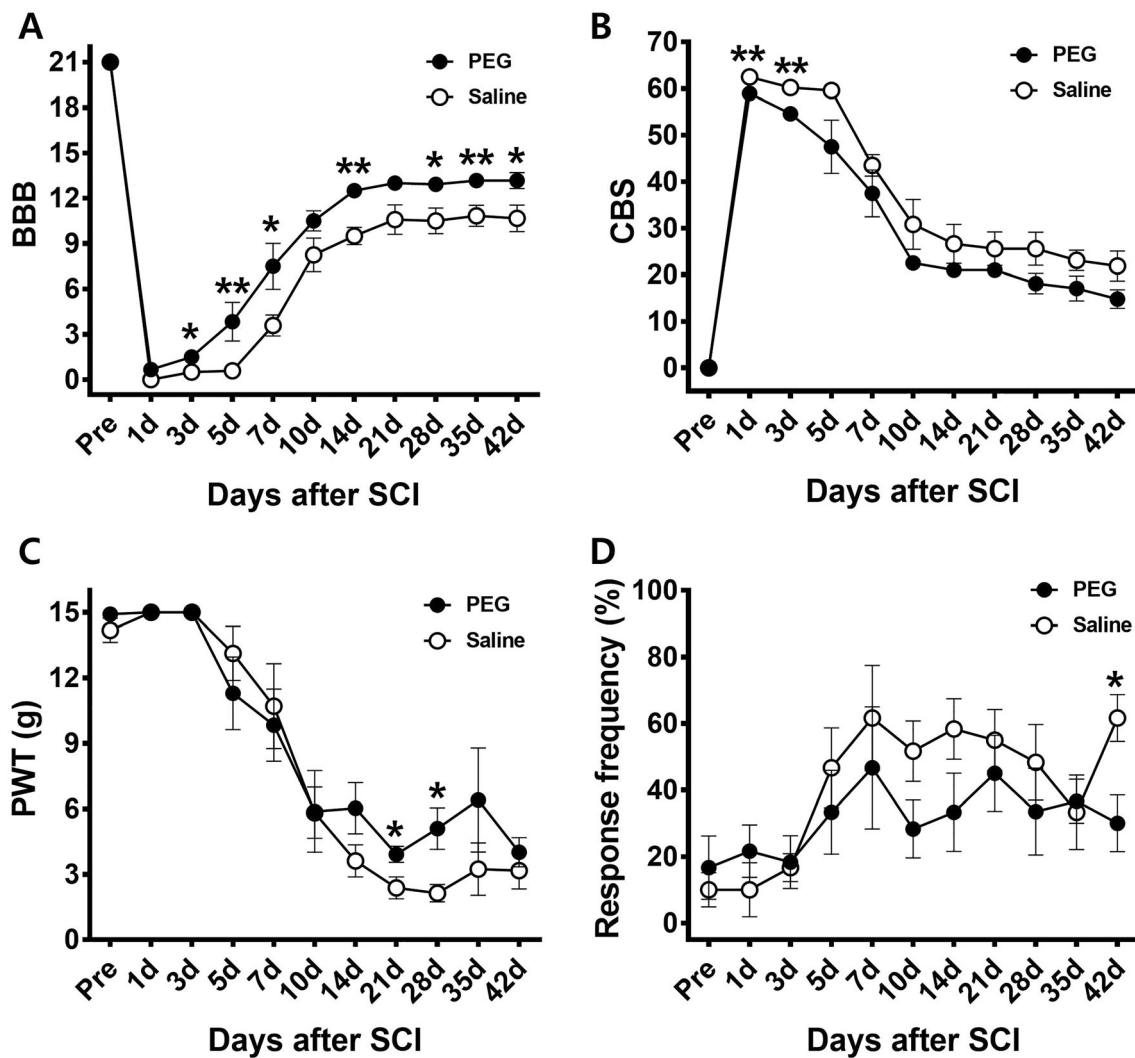


Fig. 6 Comparisons of motor and sensory functions between the PEG and saline groups. **A** Basso, Beattie, and Bresnahan locomotor rating scale (BBB). **B** Modified combined behavioral score (CBS). **C** Paw withdrawal threshold (PWT), and **D** cold test. All behavioral assessments were performed for 42 d after SCI. Asterisk (*) indicates

values that differ significantly between the PEG and saline groups ($p < 0.05$) and Double-Asterisk (**) indicates values that differ significantly between the PEG and saline groups ($p < 0.01$). PEG, polyethylene glycol; SCI, spinal cord injury

showed the decrease in PWT accompanied with aversive behaviors such as vocalization, paw licking, and attacking the mechanical stimulus to the plantar surface of the paw, which was considered an index of pain-related behaviors. A decrease in PWT was maintained until 42 days after SCI (Fig. 6C). The PWT in the PEG group was slightly higher than that in the saline group from 14 to 42 days; however, significant differences were observed between the two groups only at 21 and 28 days (21 d: $p = 0.041$; 28 d: $p = 0.026$). In the cold sensitivity test, the rats in the saline group showed a higher paw withdrawal response to acetone stimuli compared to the PEG group from 5 days after SCI;

however, a significant difference in response frequency was observed only at 42 days ($p = 0.026$) (Fig. 6D).

3.6 Morphometric analysis of tissue-sparing around the CST

Tissue-sparing at the epicenter was remarkably reduced after SCI in both groups due to cavitation and shrinkage, with only the rims of the axonal tissues bridging the rostral and caudal segments (Fig. 7A, B). The tissue-sparing in the PEG group was significantly greater than that observed in the saline group at 42 days after SCI ($p = 0.005$) (Fig. 7C).

4 Discussion

The present study demonstrated that PEG application immediately after SCI improved the disruption of vascular permeability and significantly reduced the infarct size. In addition, the number of blood vessels increased to rapidly replace the injured tissue. PEG application improved the recovery of motor function and also promoted spinal cord tissue-sparing. These results support our hypothesis that PEG reduces secondary injuries following SCI by protecting the vascular system.

To investigate the effects of PEG on the alteration of vascular permeability following SCI, temporal and spatial BSCB alterations were identified from the epicenter to the rostral and caudal segments, depending on the time point after SCI (Fig. 2). We analyzed the area and distance of EBD extravasation in the spinal cord to evaluate the degree of BSCB disruption. The present data demonstrated that the EBD extravasation in the spinal cord was started immediately and dramatically increased from 6 h after SCI, suggesting that BSCB breakdown was started immediately after SCI and was worsened with time after injury. The disruption of BSCB was maintained until 24 h after SCI and extended to the rostral and caudal segments. In the PEG group, however, EBD extravasation following SCI was significantly reduced compared to the saline group until 24 h after SCI in the analysis of the area (Fig. 2K). In the case of the distance of EBD extravasation, the BSCB disruption was not different between the two groups

immediately after SCI, but the extension of BSCB disruption in the saline group was faster to rostral and caudal directions compared to the PEG group. The significant differences between the two groups were found at 3 h and 6 h after SCI. At these time points, PEG significantly reduced the extension of the BSCB disruption. The distance of EBD signals in the saline group reached around the maximum distance (7 mm) from 3 h after SCI and continued until 24 h after SCI. In the PEG group, however, the distance of EBD signals reached to the maximum distance starting after 12 h following SCI. There were no significant differences in the distance between two groups at 12 and 24 h after SCI. In this study, we investigated the extension of EBD signals in 3 segments of spinal cords (T10-T12) with a total length about 7 mm that included the epicenter in the middle portion. Probably, that was the reason why there were no significant differences in the distance between two groups at 12 and 24 h after SCI. The present data could not include the whole effect of PEG on changes in the BSCB disruption over 3 segments of spinal cords. However, as seen in Fig. 2K, the area of BSCB disruptions between two groups significantly differed from 6 to 24 h after SCI, suggesting that the distances of 12 and 24 h were not saturated points. One possible mechanism for the effect of PEG on vascular permeability is its ability to control the movement of calcium ions [21, 25, 36]. The integrity of the blood–brain barrier and BSCB is significantly affected by the calcium concentration of the ECM. The tight junctions (TJ) composing the BSCB are sensitive

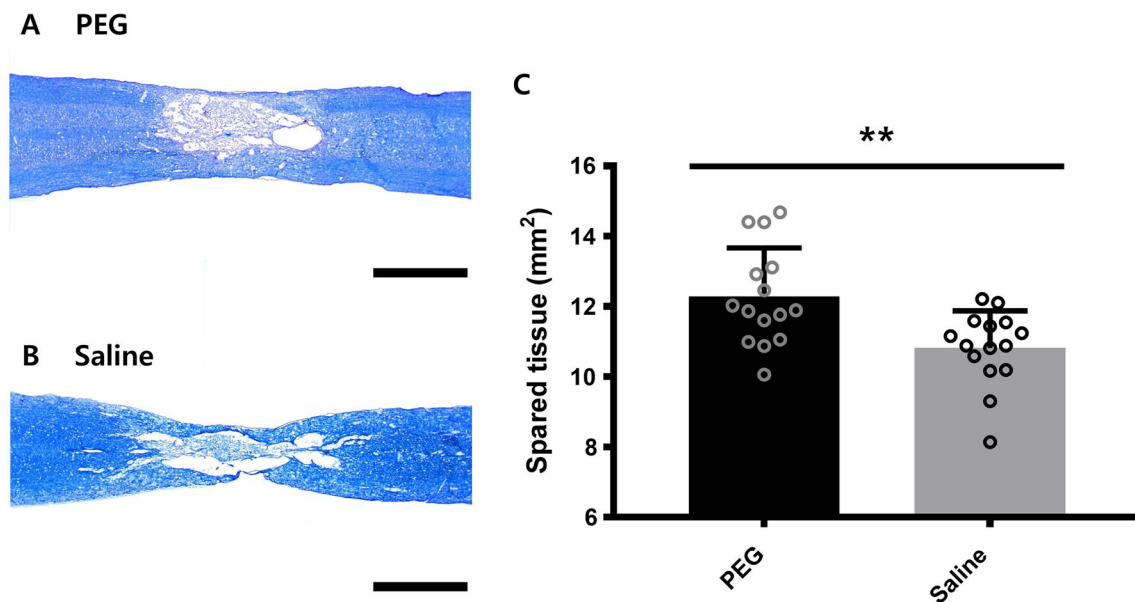


Fig. 7 Comparisons of tissue-sparing between the PEG and saline groups **A** and **B**. Tissue-sparing in the spinal cord in the PEG **A** and saline **B** groups at 42 days after SCI. **C** Area of tissue-sparing between PEG and saline groups. Asterisk (*) indicates values that

differ significantly between the PEG and saline groups ($p < 0.05$). Scale bar: **A** and **B** 2 mm. PEG, polyethylene glycol; SCI, spinal cord injury

to extracellular calcium [37] and rapid changes in extracellular calcium may lead to disruption of the tight junction affecting BSCB permeability by altering the activity of cascade signaling such as PKC [38]. Increased movement of calcium ions triggers serial destruction of the integrity of blood vessel membranes by affecting protein channels or receptors in TJ proteins [39]. A previous study demonstrated that PEG decreased intracellular calcium and oxidative stress in spinal tissues in a compressive SCI model, which supported the role of PEG in controlling the permeability of calcium ions through the cell membrane [36].

To visualize the changes in BSCB and the structure of the junctional complex of the vascular system, we stained the tissues with CD31 and ZO-1 merged with EBD signals (Fig. 3). Immediately after SCI, CD31 staining blood vessels were found at the edge of the epicenter in the white matter in both groups, and ZO-1 signals were not found near the epicenter at 0 h after SCI. EBD signals usually overlap with CD31 signals because EBD leaked from blood vessels. Increased ZO-1 signals were observed 6 h after SCI in the PEG group and merged with CD31 signals indicating the structures of the junctional complexes. These stained structures were continuously observed 24 h after SCI around the epicenter. In the saline group, the intensity of ZO-1 signals was still low and junctional structures were not found 6 h after SCI. Junctional complexes were observed around the epicenter 24 h after SCI in the saline group. This disparity can be explained by the protective effect of PEG on vascular structures. Immediate application of PEG following SCI prevents secondary damage to the vascular system and might allow the environments for the early angiogenesis. Considering the importance of junctional structures in vascular permeability to ECM [40], these results explain the drastic decrease in EBD extravasation in the PEG group from 6 to 24 h after SCI, as seen in Fig. 2. However, the analyzed areas in the saline group were farther from the epicenter than those of the PEG group because the area of injured sites where cavities or EBD signals existed was significantly different between the two groups from 6 h after SCI. Therefore, we could not quantify the phenomenon because of the different criteria and our results (Fig. 3) showed the phenomenon of vascular structures at the margin of the epicenter in the PEG and saline groups.

The BSCB disruption and change of vascular permeability initiate hemorrhage in the injured site, which is related to ischemic injury [41]. Therefore, to investigate the effect of PEG on ischemic injury, we assessed infarct size in spinal tissue by using TTC staining. TTC is a marker of metabolic activity, indicates the ischemic volume in CNS injury models, and stains the mitochondrial enzyme succinate dehydrogenase in living cells. In this study, the

spinal cord was separated into three segments because TTC cannot penetrate deep tissues from the surface. TTC staining revealed significantly reduced infarct sizes in the PEG group at 0, 6, and 24 h after SCI (Fig. 4). These results were consistent with those of BSCB function after PEG application. We observed an immediate effect of PEG on BSCB function and infarct size in the PEG group. Preserved BSCB function may affect ischemic injury by controlling hemorrhage after SCI.

Previous research demonstrated that the disruption of BSCB and the increase of vascular permeability were related to the reduction of blood vessels in the injury site [42]. Following SCI, the density of blood vessels decreased at the injury site and then significant increase in blood vessels were observed in a few days [43, 44]. To investigate the effect of PEG on the changes in blood vessels after SCI, we assessed changes in the number of blood vessels at the epicenter in both the PEG and saline groups. In the present results, a drastic increase in new blood vessels in the PEG group was observed from 6 to 24 h after SCI and rapidly replaced the epicenter when it compared to the saline group (Fig. 5). The earlier angiogenesis may result from the effect of PEG on the vascular system and spinal tissue which prevent further damage to the vascular system as shown in Fig. 2–5. According to the previous report [42], immature blood vessels forming after the injury have a higher permeability resulting from BSCB dysfunction, which can lead to leakage of inflammatory mediators or hemorrhage. However, in the present data, PEG group showed no more EBD extravasation or infarction 6 h after SCI when the blood vessels started to replace the injury site, suggesting that the newly formed blood vessels with low permeability were replaced in the injured area following SCI (Fig. 4 and 5).

Considering the importance of vascular function in spinal tissue survival, our results showing the effect of PEG on the vascular system may affect the recovery of neurological function after SCI. Bearden and Segal [45] observed the function of blood vessels as a guide for neuronal axon sprout. Other researchers have also reported the importance of blood vessels for functional recovery after SCI [46–48]. As shown in the BBB score, there was a significant difference in locomotor function between the two groups (Fig. 6), with PEG application resulting in earlier and long-lasting improvements during the experimental period. Moreover, the PEG groups also showed more tissue-sparing in the epicenter of the spinal cord around the CST. We serially sectioned the spinal tissues from the ventral to the dorsal region and grossly distinguished the location of the CST based on the shape of the gray matter in rats. Although the decrease in cavitation and shrinkage of the spinal cord after SCI did not always coincide with neurological function and functional

recovery [49], many studies have reported functional recovery with increased area of tissue sparing [49, 50], consistent with our observations of significant differences in BBB between the groups. CBS showed significant differences only in the acute phase as CBS could not discriminate the details of differences in the chronic phase. PWT was slightly increased in PEG group in the chronic phase compared to the saline group. However, there were significant differences only at 21 d and 28 d after SCI. In the cold sensitivity, a significant difference showed only at 42 d after SCI. According to the study of unilateral SCI, there was no difference in tissue-sparing between the allodynic and non-allodynic groups and it suggested that pain induced by SCI was more related to some underlying mechanism than the size or extent of the lesion [51]. Therefore, the effect of PEG on a pain processing and its underlying mechanism needs to be studied.

In the present study, the effects of PEG appeared rapidly in the vascular system and motor function after SCI. This may be possible due to the ability of low concentrations of PEG to temporarily seal the cell membranes not affected by biological factors related to cell membrane fusion [52]. While sealing the cell membrane generally requires factors such as N-ethylmaleimide-sensitive factors [53], Spaeth et al. [52] showed that low concentrations of PEG can seal cell membranes almost directly. Another possible explanation for the early improvement was that PEG also affects both neural and glial cells [21, 25, 36]. The sealing effects of PEG were mainly reported in the axonal membrane sealing of neural and glial cells after SCI. This bilateral effect of PEG may contribute to the earlier and longer-lasting improvements in functional recovery after SCI.

5 Conclusion

The present study provides preclinical evidence for the use of PEG for neuroprotection in SCI, in which one of the underlying mechanisms was the reduction of secondary injury following SCI by protecting the vascular system. However, the possible mechanism of PEG related to the reduction of vascular protection after SCI remains unknown. Further studies are needed to demonstrate the specific mechanism by which PEG protects the vascular system and spinal tissue.

Acknowledgements This work was supported by the Basic Science Research Program through the National Research Foundation of Korea (NRF) funded by the Ministry of Education, ICT & Future Planning (2019R111A2A01060115 / 2022M3C1A3090851), a grant from the Korea Health Technology R&D Project (HI21C0572) through the Korea Health Industry Development Institute (KHIDI) funded by the Ministry of Education, and Korea University Grant (K1916941).

Author contributions JL: Conceptualization, Methodology, Investigation, Formal analysis, Writing Original Draft. SCH: Formal analysis, Writing Review & Editing. HY: Investigation, Formal analysis. YWY: Conceptualization, Methodology. JK: Conceptualization, Verification, Writing Review & Editing, Supervision.

Declarations

Conflict of interest The authors declare that there is no conflict of interest.

Ethical statement All procedures were approved by the Korea University Institutional Animal Care and Use Committee (KUIA-CUC-2019-0016).

References

1. Kwon BK, Tetzlaff W, Grauer JN, et al. Pathophysiology and pharmacologic treatment of acute spinal cord injury. *Spine J*. 2004;4:451–64.
2. Povlishock JT, Christman CW. The pathobiology of traumatically induced axonal injury in animals and humans: a review of current thoughts. *J Neurotrauma*. 1995;12:555–64.
3. Sekhon LH, Fehlings MG. Epidemiology, demographics, and pathophysiology of acute spinal cord injury. *Spine*. 2001;26:S2–12.
4. Ling X, Liu D. Temporal and spatial profiles of cell loss after spinal cord injury: Reduction by a metalloporphyrin. *J Neurosci Res*. 2007;85:2175–85.
5. Liu XZ, Xu XM, Hu R, Du C, Zhang SX, McDonald JW, et al. Neuronal and glial apoptosis after traumatic spinal cord injury. *J Neurosci*. 1997;17:5395–406.
6. Blight AR. Morphometric analysis of a model of spinal cord injury in guinea pigs, with behavioral evidence of delayed secondary pathology. *J Neurol Sci*. 1991;103:156–71.
7. Popovich PG, Horner PJ, Mullin BB, Stokes BT. A quantitative spatial analysis of the blood–spinal cord barrier: I. Permeability changes after experimental spinal contusion injury. *Exp Neurol*. 1996;142:258–75.
8. Shingu H, Kimura I, Nasu Y, Shiotani A, Oh-hama M, Hijioka A, et al. Microangiographic study of spinal cord injury and myelopathy. *Paraplegia*. 1989;27:182–9.
9. Bartanusz V, Jezova D, Alajajian B, Digicaylioglu M. The blood–spinal cord barrier: morphology and clinical implications. *Ann Neurol*. 2011;70:194–206.
10. Abbott NJ, Rönnebeck L, Hansson E. Astrocyte–endothelial interactions at the blood–brain barrier. *Nat Rev Neurosci*. 2006;7:41–53.
11. Engelhardt B, Coisne C. Fluids and barriers of the CNS establish immune privilege by confining immune surveillance to a two-walled castle moat surrounding the CNS castle. *Fluids Barrier CNS*. 2011;8:4.
12. Hsu C, Hogan E, Gadsden R Sr, Spicer KM, Shi MP, Cox RD. Vascular permeability in experimental spinal cord injury. *J Neurol Sci*. 1985;70:275–82.
13. Lipton SA, Rosenberg PA. Excitatory amino acids as a final common pathway for neurologic disorders. *N Engl J Med*. 1994;330:613–22.
14. Lukáčová N, Halát G, Chavko M, Marsala J. Ischemia-reperfusion injury in the spinal cord of rabbits strongly enhances lipid peroxidation and modifies phospholipid profiles. *Neurochem Res*. 1996;21:869–73.

15. Schanne FA, Kane AB, Young EE, Farber JL. Calcium dependence of toxic cell death: a final common pathway. *Science*. 1979;206:700–2.
16. Wrathall JR, Teng YD, Choiniere D. Amelioration of functional deficits from spinal cord trauma with systemically administered NBQX, an antagonist of non-N-methyl-D-aspartate receptors. *Exp Neurol*. 1996;137:119–26.
17. Hawkins BT, Davis TP. The blood-brain barrier/neurovascular unit in health and disease. *Pharmacol Rev*. 2005;57:173–85.
18. Zlokovic BV. The blood-brain barrier in health and chronic neurodegenerative disorders. *Neuron*. 2008;57:178–201.
19. Li X, Liu KL, Li J, Tan EPS, Chan LM, Lim CT, et al. Synthesis, characterization, and morphology studies of biodegradable amphiphilic Poly[(R)-3-hydroxybutyrate]-alt-Poly(ethylene glycol) multiblock copolymers. *Biomacromol*. 2006;7:3112–9.
20. Zalipsky S. Synthesis of an end-group functionalized polyethylene glycol-lipid conjugate for preparation of polymer-grafted liposomes. *Bioconjug Chem*. 1993;4:296–9.
21. Luo J, Borgens R, Shi R. Polyethylene glycol immediately repairs neuronal membranes and inhibits free radical production after acute spinal cord injury. *J Neurochem*. 2002;83:471–80.
22. Nehrt A, Hamann K, Ouyang H, Shi R. Polyethylene glycol enhances axolemmal resealing following transection in cultured cells and in ex vivo spinal cord. *J Neurotrauma*. 2010;27:151–61.
23. Shi R, Borgens RB. Anatomical repair of nerve membranes in crushed mammalian spinal cord with polyethylene glycol. *J Neurocytol*. 2000;29:633–43.
24. Borgens RB, Shi R. Immediate recovery from spinal cord injury through molecular repair of nerve membranes with polyethylene glycol. *FASEB J*. 2000;14:27–35.
25. Baptiste DC, Austin JW, Zhao W, Nahirny A, Sugita S, Fehlings MG. Systemic polyethylene glycol promotes neurological recovery and tissue sparing in rats after cervical spinal cord injury. *J Neuropathol Exp Neurol*. 2009;68:661–76.
26. Kim J, Kim EH, Lee K, Kim B, Kim Y, Na SH, et al. Low-level laser irradiation improves motor recovery after contusive spinal cord injury in rats. *Tissue Eng Regen Med*. 2017;14:57–64.
27. Estrada V, Brazda N, Schmitz C, Heller S, Blazycza H, Martini R, et al. Long-lasting significant functional improvement in chronic severe spinal cord injury following scar resection and polyethylene glycol implantation. *Neurobiol Dis*. 2014;67:165–79.
28. Saria A, Lundberg JM. Evans blue fluorescence: quantitative and morphological evaluation of vascular permeability in animal tissues. *J Neurosci Methods*. 1983;8:41–9.
29. Li ZW, Zhao JJ, Li SY, Cao TT, Wang Y, Guo Y, et al. Blocking the EGFR/p38/NF- κ B signaling pathway alleviates disruption of BSCB and subsequent inflammation after spinal cord injury. *Neurochem Int*. 2021;150: 105190.
30. Lee JY, Choi HY, Ahn HJ, Ju BG, Yune TY. Matrix metalloproteinase-3 promotes early blood–spinal cord barrier disruption and hemorrhage and impairs long-term neurological recovery after spinal cord injury. *Am J Pathol*. 2014;184:2985–3000.
31. Casella GTB, Marcillo A, Bunge MB, Wood PM. New vascular tissue rapidly replaces neural parenchyma and vessels destroyed by a contusion injury to the rat spinal cord. *Exp Neurol*. 2002;173:63–76.
32. Basso DM, Beattie MS, Bresnahan JC. A sensitive and reliable locomotor rating scale for open field testing in rats. *J Neurotrauma*. 1995;12:1–21.
33. Gale K, Kerasidis H, Wrathall JR. Spinal cord contusion in the rat: behavioral analysis of functional neurologic impairment. *Exp Neurol*. 1985;88:123–34.
34. Dixon W. Staircase bioassay: the up-and-down method. *Neurosci Biobehav Rev*. 1991;15:47–50.
35. Choi Y, Yoon YW, Na HS, Kim SH, Chung JM. Behavioral signs of ongoing pain and cold allodynia in a rat model of neuropathic pain. *Pain*. 1994;59:369–76.
36. Luo J, Borgens R, Shi R. Polyethylene glycol improves function and reduces oxidative stress in synaptosomal preparations following spinal cord injury. *J Neurotrauma*. 2004;21:994–1007.
37. Brown RC, Davis TP. Calcium modulation of adherens and tight junction function: a potential mechanism for blood-brain barrier disruption after stroke. *Stroke*. 2002;33:1706–11.
38. Balda MS, Gonzalez-Mariscal L, Matter K, Cerejido M, Anderson JM. Assembly of the tight junction: the role of diacylglycerol. *J Cell Biol*. 1993;123:293–302.
39. Simard JM, Tsybalyuk O, Ivanov A, Ivanova S, Bhatta S, Geng Z, et al. Endothelial sulfonylurea receptor 1–regulated NC CA-ATP channels mediate progressive hemorrhagic necrosis following spinal cord injury. *J Clin Invest*. 2007;117:2105–13.
40. Bazzoni G, Dejana E. Endothelial cell-to-cell junctions: molecular organization and role in vascular homeostasis. *Physiol Rev*. 2004;84:869–901.
41. Losey P, Young C, Krimholtz E, Bordet R, Anthony DC. The role of hemorrhage following spinal-cord injury. *Brain Res*. 2014;1569:9–18.
42. Figley SA, Khosravi R, Legasto JM, Tseng YF, Fehlings MG. Characterization of vascular disruption and blood–spinal cord barrier permeability following traumatic spinal cord injury. *J Neurotrauma*. 2014;31:541–52.
43. Imperato-Kalmar EL, McKinney RA, Schnell L, Rubin BP, Schwab ME. Local changes in vascular architecture following partial spinal cord lesion in the rat. *Exp Neurol*. 1997;145:322–8.
44. Beggs JL, Waggenger JD. Microvascular regeneration following spinal cord injury: the growth sequence and permeability properties of new vessels. *Adv Neurol*. 1979;22:191–206.
45. Bearden SE, Segal SS. Microvessels promote motor nerve survival and regeneration through local VEGF release following ectopic reattachment. *Microcirculation*. 2004;11:633–44.
46. Patel CB, Cohen DM, Ahobila-Vajjula P, Sundberg LM, Chacko T, Narayana PA. Effect of VEGF treatment on the blood–spinal cord barrier permeability in experimental spinal cord injury: dynamic contrast-enhanced magnetic resonance imaging. *J Neurotrauma*. 2009;26:1005–16.
47. Herrera JJ, Sundberg LM, Zentilin L, Giacca M, Narayana PA. Sustained expression of vascular endothelial growth factor and angiopoietin-1 improves blood–spinal cord barrier integrity and functional recovery after spinal cord injury. *J Neurotrauma*. 2010;27:2067–76.
48. Widenfalk J, Lipson A, Jubran M, Hofstetter C, Ebendal T, Cao Y. Vascular endothelial growth factor improves functional outcome and decreases secondary degeneration in experimental spinal cord contusion injury. *Neuroscience*. 2003;120:951–60.
49. Hodgetts SI, Simmons PJ, Plant GW. Human mesenchymal precursor cells (Stro-1⁺) from spinal cord injury patients improve functional recovery and tissue sparing in an acute spinal cord injury rat model. *Cell Transplant*. 2013;22:393–412.
50. Patel SP, Sullivan PG, Lyttle TS, Magnuson DSK, Rabchevsky AG. Acetyl-L-carnitine treatment following spinal cord injury improves mitochondrial function correlated with remarkable tissue sparing and functional recovery. *Neuroscience*. 2012;210:296–307.
51. Detloff MR, Wade RE Jr, Houlié JD. Chronic at-and below-level pain after moderate unilateral cervical spinal cord contusion in rats. *J Neurotrauma*. 2013;30:884–90.
52. Spaeth CS, Robison T, Fan JD, Bittner GD. Cellular mechanisms of plasmalemmal sealing and axonal repair by polyethylene glycol and methylene blue. *J Neurosci Res*. 2012;90:955–66.
53. Whiteheart S, Schraw T, Matveeva EA. N-ethylmaleimide sensitive factor (NSF) structure and function. *Int Rev Cytol*. 2001;207:71–112.

Publisher's Note Springer Nature remains neutral with regard to jurisdictional claims in published maps and institutional affiliations.

Springer Nature or its licensor (e.g. a society or other partner) holds exclusive rights to this article under a publishing agreement with the author(s) or other rightsholder(s); author self-archiving of the accepted manuscript version of this article is solely governed by the terms of such publishing agreement and applicable law.